Direct Rheological Evidence of Monomer Density Reequilibration for Entangled Polymer Melts

Chen-Yang Liu,*,†,‡ Roland Keunings,§ and Christian Bailly†

Unité de Chimie et de Physique des Hauts Polymères, Université catholique de Louvain, B-1348 Louvain-La-Neuve, Belgium, Key Laboratory of Engineering Plastics, Joint Laboratory of Polymer Science and Materials, Institute of Chemistry, Chinese Academy of Sciences, Beijing 100080, China, and CESAME, Université catholique de Louvain, B-1348 Louvain-La-Neuve, Belgium

Received November 23, 2006; Revised Manuscript Received February 16, 2007

ABSTRACT: The monomer density reequilibration relaxation is directly observed for the first time from the linear viscoelastic data of very high molecular weight linear polybutadiene, polyisobutene and polyisoprene. We use a simple procedure of subtracting contributions of the high-frequency Rouse-like modes from the experimental curves. The stress decay of the monomer redistribution process is characterized by a single exponential (Maxwell form), and the observed relaxation strength is one-fourth of the plateau modulus. Moreover, the characteristic relaxation time is close to the equilibration time τ_e of an entanglement segment. The observed reequilibration dynamics appears to be independent of polymer species. The high-frequency relaxation modes can be reconstructed as a superposition of power law Rouse-like dynamics and Maxwell monomer reequilibration. The dynamic moduli curves calculated in this way show excellent agreement with the experimental results in the high-frequency region. We further propose a possible "experimental definition" for τ_e. It corresponds to an easily observable cross-point between the extended plateau modulus and the power law region of the loss modulus.

Downloaded by UNIV CATHOLIQUE DE LOUVAIN on October 15, 2009 | http://pubs.acs.org
Publication Date (Web): March 24, 2007 | doi: 10.1021/ma062695f

Introduction

Linear viscoelasticity (LVE) is an essential aspect of polymer rheological behavior[1] as it reflects the distribution of relaxation times, which is in turn strongly related to the molecular structure, i.e., molecular weight (MW), molecular weight distribution (MWD), and molecular architecture (star, H-, comb, ring, ...).[2−5] Hence, LVE provides fundamental insights on the link between polymer structure and dynamics. In the frame of popular "tube" models, the main relaxation in the terminal region is identified with a curvilinear "reptation" of the chains in the entanglement network. This is equivalent to considering the motion of a polymer molecule in a "tube", representing the topological constraints imposed by the surrounding chains.[6,7] For quantitative agreement, two additional relaxation mechanisms must be accurately taken into consideration,[8] i.e. "constraint release" (CR) representing the mutual influence of relaxing chains[9,10] and "contour-length fluctuations" (CLF) describing springlike motions of the chain-ends.[11,12]

At short times, or equivalently high frequencies, the corresponding fast motions of entangled polymer chains are usually described by the Rouse model.[1,13] A distinction is classically made between the very fast dynamics of entanglement segments themselves and the redistribution of segments along the tube. The latter are constrained by the presence of the tube ("one-dimensional" Rouse model), while the former are not. Alternatively, this redistribution or reequilibration of monomer density can be pictured as a sliding motion of monomers through slip-links. Hence, after a step deformation which disturbs the monomer density along the tube, an entangled chain in the melt or solution can return to the equilibrium situation, as opposed to a covalently cross-linked network.

In the theory of rubber elasticity, the plateau stress tensor $\boldsymbol{\sigma}$ can be linked to the average chain conformation as follows[14]

$$\boldsymbol{\sigma} = \frac{3\rho RT}{M_e}\mathbf{Q} + p\boldsymbol{\delta} \tag{1}$$

with $\mathbf{Q}$ being the conformation tensor

$$\mathbf{Q} = \langle(\mathbf{E}\cdot\mathbf{u})(\mathbf{E}\cdot\mathbf{u})\rangle - \frac{1}{3}\boldsymbol{\delta} \tag{2}$$

where ρ is the polymer density, R is the gas constant, T is the absolute temperature, M_e is the molecular weight between two entanglement points, $\mathbf{E}$ is the step deformation tensor, $\mathbf{u}$ is the tangent unit vector along the chain, p is the pressure, and $\boldsymbol{\delta}$ is the unit tensor. The bracket represents the usual average over all segmental orientations. Hence the stress derives from segmental stretch (since $|\mathbf{E}.\mathbf{u}|$ is larger than unity) as well as orientation.

In contrast, because of the existence of monomer density reequilibration, the stress for an entangled melt is modified by Doi and Edwards with the tensor $\mathbf{Q}'$ replacing $\mathbf{Q}$ in eq 1 and given as[7]

$$\mathbf{Q}' = \left\langle\frac{(\mathbf{E}\cdot\mathbf{u})(\mathbf{E}\cdot\mathbf{u})}{|\mathbf{E}\cdot\mathbf{u}|}\right\rangle / \langle|\mathbf{E}\cdot\mathbf{u}|\rangle - \frac{1}{3}\boldsymbol{\delta} \tag{3}$$

The form of the conformation tensor $\mathbf{Q}'$ ensures that only the orientation of the chain contributes to the stress. Therefore, the "equilibrated" plateau stress for the entanglement network is smaller than the corresponding value for the cross-linked network with the same cross-linking density. The idea that entanglements behave as slip links can be validated by stretching experiments of lightly cross-linked rubbers, which show a stress softening in the low deformation regime and a hardening in

* Corresponding author. E-mail: liucy@poly.ucl.ac.be.
† Unité de Chimie et de Physique des Hauts Polymères, Université catholique de Louvain.
‡Key Laboratory of Engineering Plastics, Joint Laboratory of Polymer Science and Materials, Institute of Chemistry, Chinese Academy of Sciences.
§CESAME, Université catholique de Louvain.

10.1021/ma062695f CCC: $37.00 © 2007 American Chemical Society
Published on Web 03/24/2007

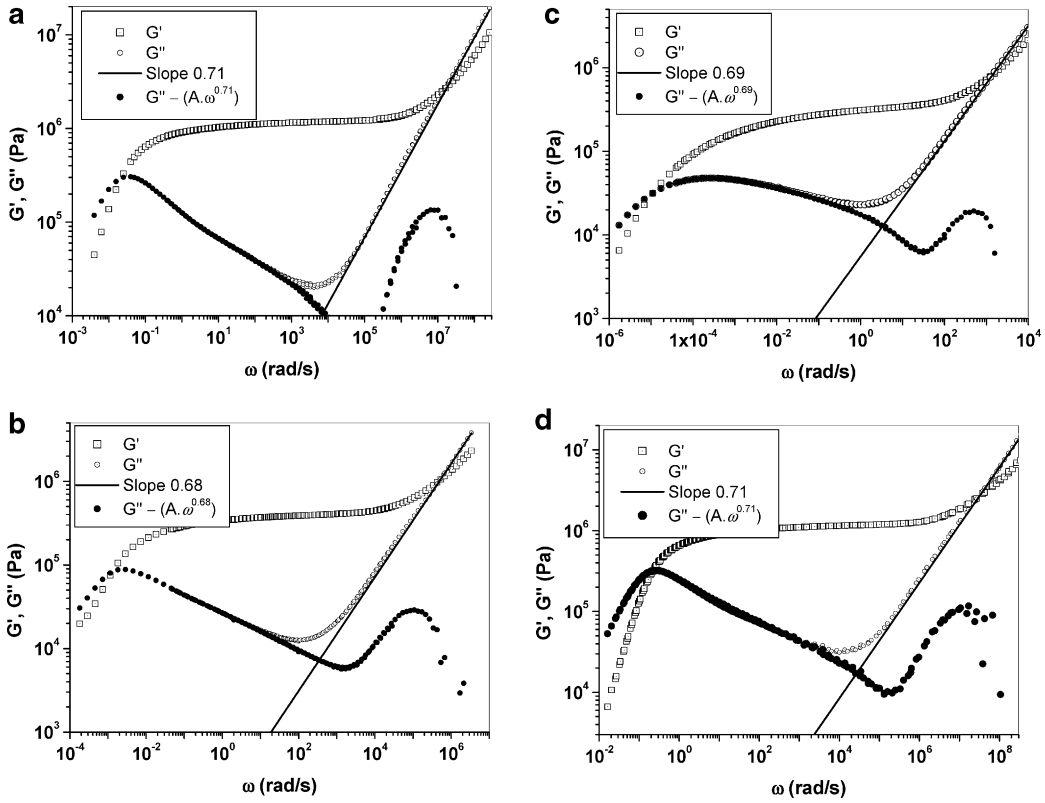

Figure 1. Master curves at 25 °C. Open symbols: original LVE data; filled symbol: G'' data from which the contributions of the high-frequency power law relaxation are subtracted; straight line: power law corresponding to the high-frequency relaxation. Key: (a) PBD-1.2M with a slope of 0.71; (b) PI-1.3M with a slope of 0.68; (c) PIB-2.6M with a slope of 0.69; (d) PBD-410K with a slope of 0.71 at 40 °C.

the high deformation regime in the well-known Mooney−Rivlin plot. The former is dominated by chain slippage; the latter is due to the inextensibility of cross-linked segments at high deformations.[15]

Lin[16] has assumed, already in the eighties, that chain sliding motions involve several entanglement segments, that the corresponding relaxation strength is $^1/_4$ of the plateau modulus G_N^0 and that the decay toward equilibrium is characterized by a single exponential. Likhtman and McLeish[12] have recently presented a different theoretical analysis of this phenomenon, which they describe as "longitudinal modes" of the stress relaxation. According to Likhtman and McLeish, monomer redistribution along the tube after a deformation relaxes $^1/_5$ of the stress (equivalently, $^1/_4$ of the plateau modulus) and the process extends between τ_e, the Rouse time of one entanglement segment, and τ_R, the Rouse time of the whole chain. Other models predict different values for the monomer redistribution relaxation strength. The Milner−McLeish[17] tube model predicts $^1/_3$. The Rubinstein and Panyukov network model[18] predicts $^3/_7$. It is also worth noting that recent slip-link simulations find that the equilibrated moduli of cross-linked and slip-link networks differ by a factor of $^4/_5$.[19]

However, to our knowledge, no clear *experimental* rheological evidence (the relaxation strength, the characteristic relaxation time, and the relaxation form) of the "monomer density reequilibration" or "longitudinal modes" has yet been presented in the literature, since these dynamics are very subtle and locate between the terminal relaxation and the high-frequency Rouse-like relaxation, which significantly overlap for polymers with typical MW. In the present paper, we detect, for the first time, the relaxation process corresponding to monomer density reequilibration by analyzing the linear viscoelastic response of very high MW monodisperse polymers in order to achieve the required frequency separation of the different relaxations.

Experiments

Very high MW narrow disperse 1,4-polybutadiene (PBD-1.2M: $M_w = 1240$ kg/mol, $M_w/M_n = 1.13$, $M_w/M_e \sim 793$), 1,4-polyisoprene (PI-1.3M: $M_w = 1310$ kg/mol, $M_w/M_n = 1.1$, $M_w/M_e \sim 278$), and polydisperse polyisobutylene (PIB-2.6 M: $M_v = 2600$ kg/mol, $M_v/M_n = 6.1$, $M_v/M_e \sim 456$) were used for linear viscoelasticity measurements in this study. The measurements were made using a TA ARES rheometer with 8 mm diameter parallel-plate geometry to avoid the instruments compliance problem for high moduli (or high stiffness of samples).[20] Because all samples have very long terminal relaxation times, special care was taken to ensure optimal loading of the samples. The TA Orchestrator software was used to derive master curves at a reference temperature of 25 °C with the help of a two-dimensional residual minimization technique. The details of samples and LVE measurements have been described before.[21,22] Rheological data of PBD-410K ($M_w = 410$ kg/mol, $M_w/M_n = 1.01$, $M_w/M_e \sim 262$) at 40 °C have been kindly supplied by Prof. Wang from Akron University to provide an independent check and comparison with published data.[23]

Results and Discussion

Separations of the Different Relaxation Modes. The master curves are presented in Figure 1 for all samples. Because the number of entanglements Z is very large, the terminal relaxation and the fast Rouse-like relaxation are well separated for all polymers, e.g., the values of G'_{min} are much higher than the values of G''_{min} at the frequency ω_{min} where G'' reaches a minimum, and the terminal relaxation peaks are clearly identified. Among the polymers under study, PBD-1.2M has the highest Z value (about 750 since the molar mass between entanglement for polybutadiene $\sim$ 1600 g/mol). Hence, the terminal and Rouse-like relaxations are *fully* separated in that case (the ratio G'_{min}/G''_{min} is about 100, as shown in Figure 1a) and the interference between the terminal peak and the high-frequency relaxation modes can be neglected. Figure 1a clearly

Downloaded by UNIV CATHOLIQUE DE LOUVAIN on October 15, 2009 | http://pubs.acs.org
Publication Date (Web): March 24, 2007 | doi: 10.1021/ma062695f

Downloaded by UNIV CATHOLIQUE DE LOUVAIN on October 15, 2009 | http://pubs.acs.org
Publication Date (Web): March 24, 2007 | doi: 10.1021/ma062695f

shows that the high-frequency relaxation region of PBD-1.2M is dominated by a power law behavior *over more than three decades* of frequency, with an experimental slope of 0.71. For polyisoprene and polyisobutene, the slope is slightly lower (0.68 and 0.69 respectively, see Figure 1, parts b and c).

The experimental exponent for G'' in the transition zone from the rubbery plateau to the glassy plateau is significantly larger than that expected from the Rouse model ($\propto\omega^{0.5}$) in most cases. This is already reported by Ferry for poly(*n*-octyl methacrylate) (ref 1, p 343, Figure 12-9) and high MW PIB (1560 kg/mol; ref 1, p 606, data in the table). Colby, Fetters and Graessley (ref 24, Figure 7) clearly point out that the shape of G' and G'' is certainly not consistent with the Rouse model for PBD since the G'' slope is larger than 0.5 not only above the $G'-G''$ crossover but also below it for G''. The continuity of the G'' slope below (frequency-wise) the second crossover is very significant. Indeed, while it can be argued that the quality of the experimental data can be affected by compliance problems[20] in the very stiff region above the crossover, this cannot be true below the crossover.

Whether specific interchain interactions (hydrodynamic interactions) or intrachain effects (local stiffness) play the key role to explain the discrepancy with the Rouse model, is unclear so far. For example, Smith et al.[25] show by analyzing neutron scattering experiments that "Rouse-type analytical models fail to account for this non-Gaussianity leading to large deviations between the experimental dynamic structure factor and model predictions". On the other hand, Harnau et al.[26] argue that local stiffness effects play an important role for the failure of the Rouse model. More experimental work and theoretical analysis is needed to resolve these issues. In summary, the Rouse model does not work quantitatively in the transition zone for entangled polymer melts. There is no consensus at the moment on the molecular interpretation of this discrepancy. However, extensive and consistent rheological data on high MW samples show a distinct single power law region over a very broad frequency range above and below the $G'-G''$ crossover. The exact exponent is slightly dependent on the polymer but is always higher than the Rouse exponent. In the remainder of the paper, we will only use the term "*high-frequency power law relaxation*" without reference to the Rouse model.

Closer examination of Figure 1 reveals that the experimental G'' curves present a small shoulder at frequencies just below the frequency where G' and G'' have a cross-point. Because minute details can always be questioned on master-curves, as there is unavoidable residual uncertainty due to the superposition procedure, we have also examined the single temperature data for PBD-1.2M at −80 °C (corresponding to high-frequency data in the master curve). The results are presented in Figure 2a. The small peak is clearly visible. There are two ways to highlight its presence. First, the G'' data can be *divided* by the power law. The resulting peak is shown in Figure 2b. A second method is to *subtract* the power law from the G'' data (Figure 2c). Again, a peak is detected. The same results can be observed as well from data at −85 °C, as reported in Figure 2, parts d and e.

Figure 3a shows that the loss modulus of PBD-1.2M closely follows the power law over more than 3 decades and the "baseline" is clearly visible *above as well as below* the high-frequency peak (see also Figure 2, parts a and d). Therefore, it makes sense to subtract the contribution of the corresponding high-frequency power law relaxation from the experimental curve with an experimental exponent 0.71. We are encouraged to follow this procedure based on the strong experimental evidence of a single slope *on both sides of* the crossover point. On the high-frequency side, there is little doubt about the validity of the observed power law, despite the discrepancy with existing models. Indeed, interference with glassy modes, which would significantly complicate the analysis, is unlikely since the system is still far removed from the glass transition. Indeed, G' does not exceed 10^7 Pa at 10^8 rad/s, well above the peak in Figure 3a. In addition, with 8 mm plates, we have recently shown that compliance problems are negligible when G^* is below 4×10^7 Pa.[20] On the low-frequency side, we simply follow the experimental evidence again, despite the inconsistency with theory.

After subtraction of the high-frequency power law relaxation spectrum, the G'' data (filled cycle in Figure 1a) exhibit two relaxation peaks, which correspond to the terminal peak and the new high-frequency relaxation, respectively. The linear−log plot in Figure 3b clarifies the situation. Indeed, the two peaks are completely separated for PBD-1.2M. Furthermore, parts c, d, and e of Figure 3 (also in the log−log plots of Figures 1b−d) clearly show that a new relaxation peak appears at high frequencies for all the samples tested, when using the same subtraction procedure (with slightly different power law exponents adjusted to the experimental curves: 0.68−0.71).

Relaxation Strength of the High-Frequency Peak. Thanks to the excellent separation of the terminal and the high-frequency relaxations, the respective relaxation strengths can be calculated by numerical integration over the corresponding loss moduli, based on the Kronig−Kramers relation:

$$G^0_{\text{peak}} = \frac{2}{\pi}\int G''_{\text{peak}}(\omega)\, \mathrm{d}(\ln\omega) \tag{4}$$

with G^0_{peak} the difference between G' moduli above and below the transition. The integral values of the terminal peak ($G^0_{\text{term}} = 1.15$ MPa) and the high-frequency peak ($G^0_{\text{HF}} = 0.26$ MPa) also are shown in Figure 3b. As expected, the value of G^0_{term} is equal to the experiment plateau modulus $G_N{}^0$ of PBD (1.16 MPa).[21] On the other hand, the integral area of the high peak is about $^1/_4$ of the area of the terminal peak for PBD-1.2M. The results for the other samples are consistent with this ratio, although it is difficult to obtain quantitative conclusions from Figure 3c−e because of the incomplete separation of the terminal peak and the high-frequency peak.

This experimental observation strongly suggests that the high-frequency peak is indeed associated with the monomer redistribution process, since it is located on the frequency scale in the vicinity of the second crossover, i.e., around $1/\tau_e$, and the relaxation strength is consistent with well-known predictions[7] for the ratio between plateau stresses of cross-linked rubbers and entangled melts. Apparently, the monomer reequilibration process is responsible for the relaxation of $^1/_5$ of the stress initially stored in the entangled network. It is a rather intriguing result, because whereas the Lin[16] and Likhtman−McLeish models[12] predict the same value, they use very different relaxation forms, which will be discussed later. The factor $^1/_5$ is in excellent agreement with recent slip-link simulations, which find that the equilibrated moduli of cross-linked and slip-link networks differ by a factor of $^4/_5$.[19] Moreover, other models predict quite different ratios.[17,18]

Characteristic Relaxation Time of the High-Frequency Monomer Reequilibration Peak. On the basis of the discussion above, $1/\omega_{\text{max\_reeq}}$, with $\omega_{\text{max\_reeq}}$ the angular frequency where the subtracted G'' peak reaches a maximum, must be a characteristic time of the monomer reequilibration process. The angular frequency $\omega_{\text{max\_reeq}}$ is very close the $\omega_{G''-G_N{}^0}$ where G'' is equal to $G_N{}^0$, or $\omega_{G'-G''}$ where G' and G'' have their second

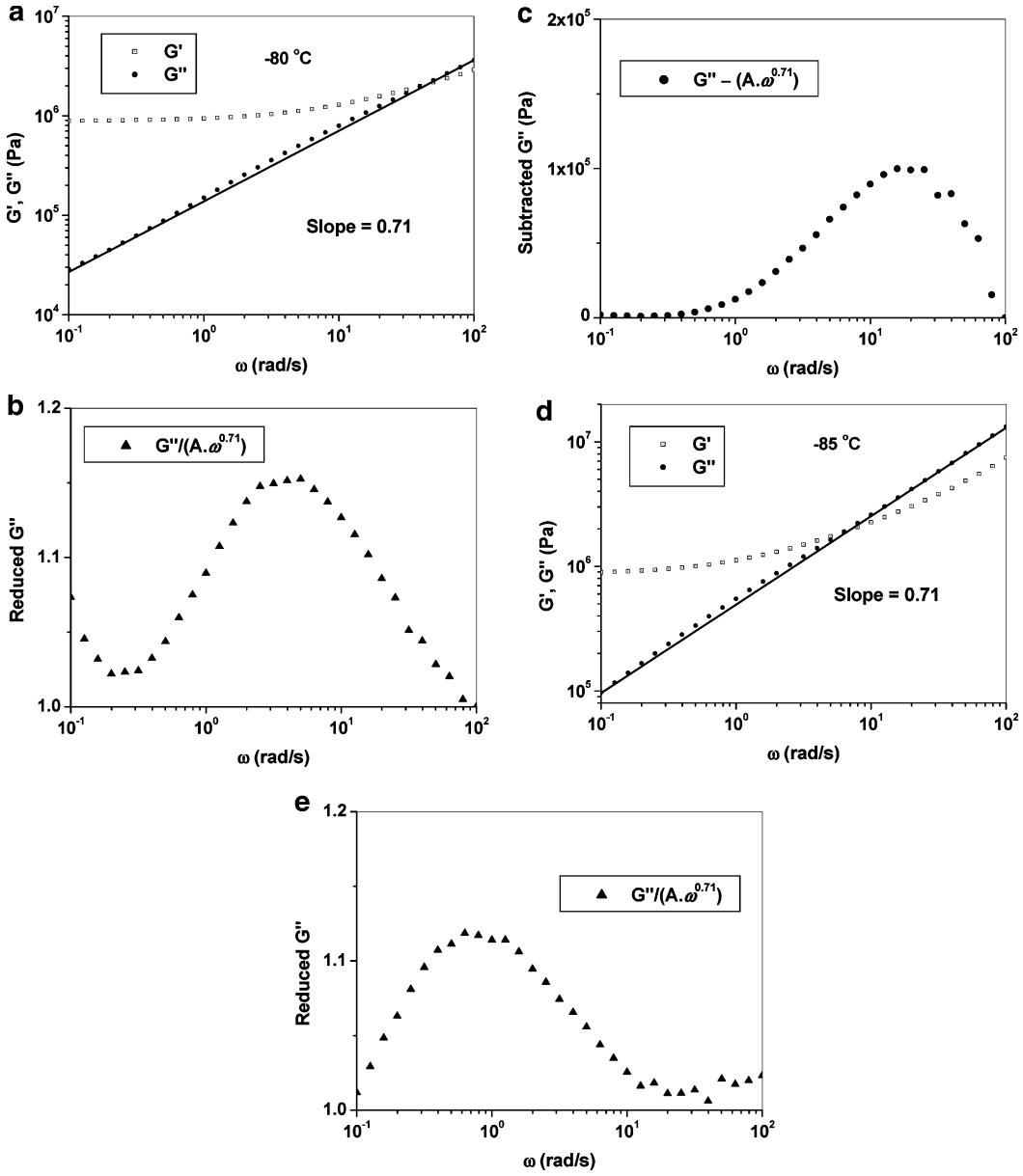

Figure 2. (a) LVE data of PBD-1.2M at −80 °C. A straight line represents the high-frequency power law. (b) Reduced G'' at −80 °C. Original G'' data are divided by ($A\omega^{0.71}$). (c) Subtracted G'' at −80 °C. Power law ($A\omega^{0.71}$) subtracted from original G'' data. (d) LVE data of PBD-1.2M at −85 °C. A straight line represents the high-frequency power-law. (e) Reduced G'' at −85 °C. Original G'' data are divided by ($A\omega^{0.71}$).

Downloaded by UNIV CATHOLIQUE DE LOUVAIN on October 15, 2009 | http://pubs.acs.org
Publication Date (Web): March 24, 2007 | doi: 10.1021/ma062695f

cross-point, as shown in Figure 3a. The experimental values of the three characteristic frequencies for all samples are reported in Table 1. The ratios $\omega_{G''-G_N^0}/\omega_{\max\_reeq}$ and $\omega_{G'-G''}/\omega_{\max\_reeq}$ are also listed in Table 1. A common behavior is observed: the $\omega_{G''-G_N^0}/\omega_{\max\_reeq}$ ratio is close to 1 and the $\omega_{G'-G''}/\omega_{\max\_reeq}$ ratio is close to 3 for all samples. Therefore, all three times scale in the same way and should logically be very close to τ_e. An accurate determination of τ_e (or equivalently of the monomer friction coefficient, ζ_0) is an important subject that remains controversial.

The most accurate method is to measure the kinematic viscosity of short chains below M_c, the critical molecular weight.[24] The monomer friction coefficient, ζ_0, can be evaluated from the Rouse model expression for kinematic viscosity. This method is very complex, since the kinematic viscosities of several short chains lengths must be obtained and adjusted to constant monomer friction coefficient. The second method is to fit the dynamic moduli at high frequencies by the Rouse model. However, Colby et al.[24] previously pointed out that the shape of G' and G'' is certainly not Rouse-like (Figure 7 in ref 24), and values of ζ_0 deduced from the two procedures have been found to disagree by a factor up to 3. The third method is to identify τ_e by comparison of the experimental terminal properties with corresponding values predicted with the help of a tube model. However, the validity of the extracted parameter is critically dependent on the accuracy of the model and the magnitude of τ_e can differ by a factor of about 3.0 for different tube theories.[27] A comparison of τ_e values reported in literature for 1,4-PBD is presented in Appendix A. For both the "Rouse" and the "tube model" methods, the discrepancy between the predicted and experimental high-frequency slopes of the dynamic moduli remains a significant issue and explains the large uncertainty on τ_e. For instance, the sophisticated Likhtman−McLeish tube model[12] predicts two distinct slopes for G'' in the high-frequency region: a classical 0.5 Rouse slope above the second $G'-G''$ cross-point, corresponding to unhindered Rouse motions of segments shorter than the entanglement length, and an average 0.7 slope below the cross-point (changes slightly with frequency: refer to Figure 7a in ref 12), corresponding to the tube-constrained Rouse motions of segments longer than

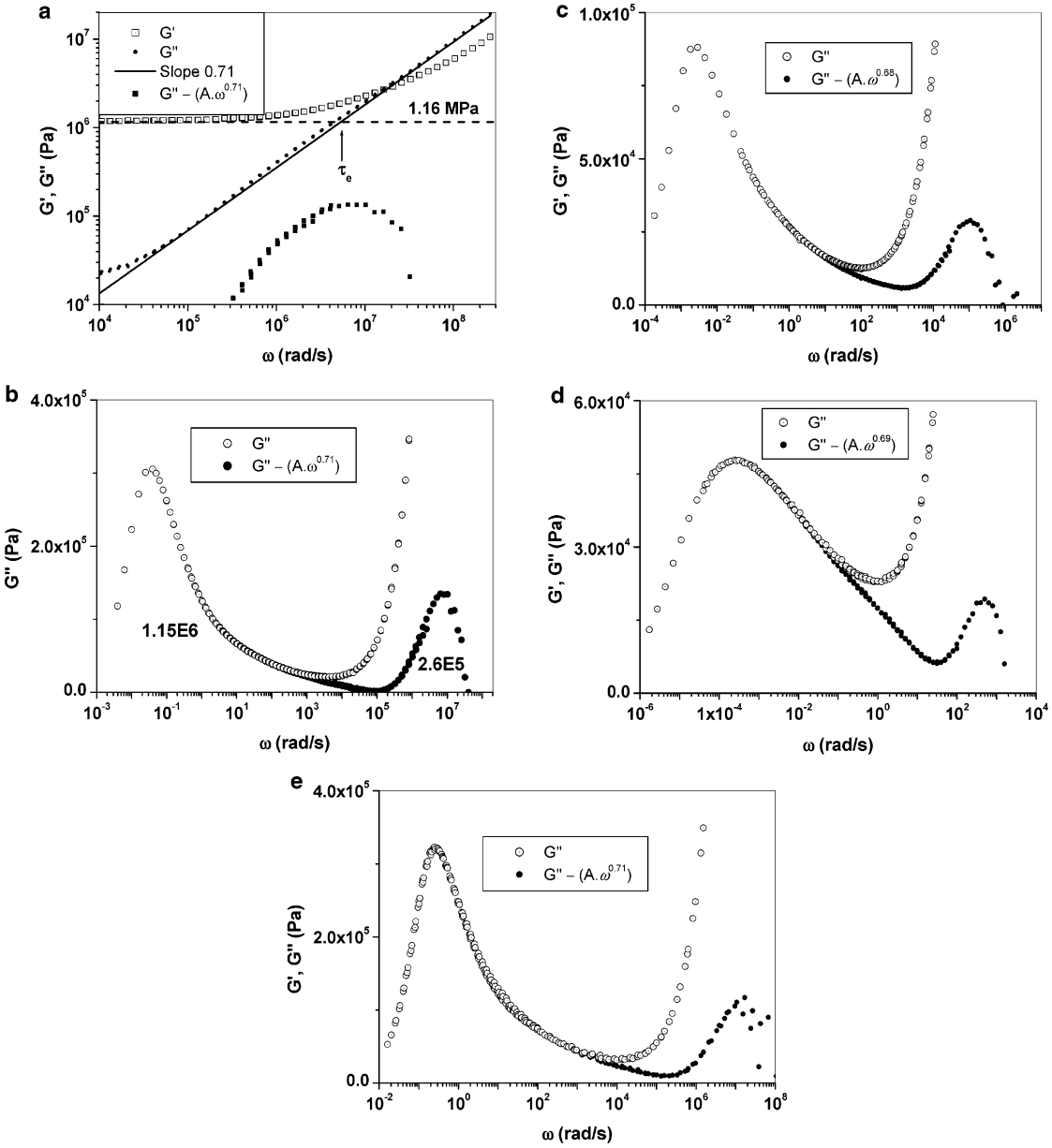

Figure 3. (a) High-frequency region of PBD-1.2M. Dashed line is the plateau modulus $G_N^0 = 1.16$ MPa. The experimental equilibration time τ_e is defined as the cross point between G'' and G_N^0. (b) Linear−log plot corresponding Figure 1a. The integral areas of the terminal peak and the reequilibration peak calculated from eq 4 are 1.15 and 0.26 MPa, respectively. (c) Linear−log plot corresponding Figure 1b. (d) Linear−log plot corresponding to Figure 1c. (e) Linear−log plot corresponding to Figure 1d.

Table 1. Characteristic Frequencies (rad/s) and Ratios

sample	ω_{max_reeq}	$\omega_{G''-G_N^0}$	$\omega_{G'-G''}$	ratio of $\omega_{G''-G_N^0}/\omega_{max\_reeq}$	ratio of $\omega_{G'-G''}/\omega_{max\_reeq}$
PBD-1.2M	6.5×10^6	5.4×10^6	1.9×10^7	0.83	2.9
PI-1.3M	1.15×10^5	1.25×10^5	4.5×10^5	1.1	3.9
PIB-2.6M	420	380	1300	0.90	3.1
PBD-410K	1.07×10^7	9.7×10^6	3×10^7	0.91	2.8

the entanglement length. This double slope is clearly inconsistent with the wide frequency range single slope actually observed in Figure 1a−d. Because of the discrepancy between existing models and experiments in the high-frequency region, model-independent determinations of the fundamental scaling parameter τ_e remain very desirable. The monomer redistribution relaxation peak appears to offer such an opportunity because the reequilibration process is governed mainly by τ_e. Moreover, the location of the peak is very close the cross point between the extended plateau and G'' in the power law region (refer to Figure 3a). This provides a convenient method for a model-independent experimental determination of τ_e.

Shape of the High-Frequency Monomer Reequilibration Peak. The monomer redistribution peak is quite narrow by comparison with the terminal peak (refer to Figure 1a−d and Figure 3b,c). For example, the integral area of the redistribution peak, G^0_{reeq} is about 0.26 MPa, while the value of G'' at the maximum, G''_{max}, is around 0.135 MPa for PBD-1.2M. Therefore, ratio of G^0_{reeq}/G''_{max}, reflecting the width of the peak, is about 2. This is typical for a Maxwell peak. The corresponding

Downloaded by UNIV CATHOLIQUE DE LOUVAIN on October 15, 2009 | http://pubs.acs.org
Publication Date (Web): March 24, 2007 | doi: 10.1021/ma062695f

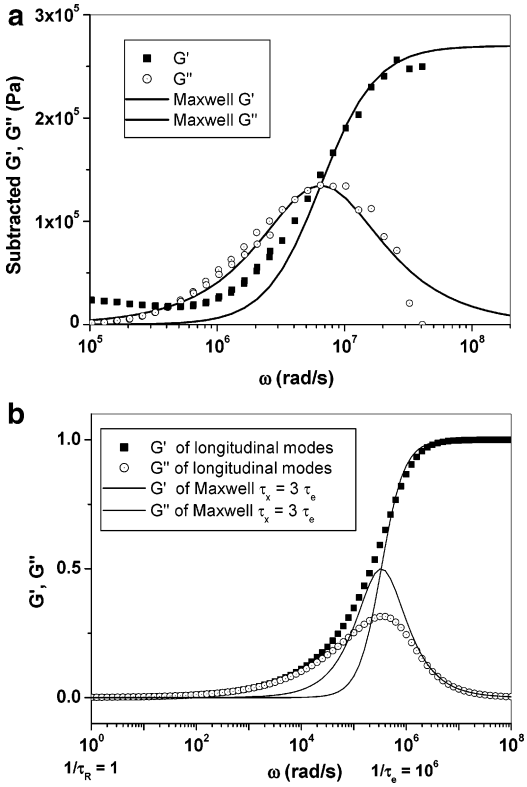

Figure 4. (a) Monomer reequilibration relaxation (subtracted from master curve of PBD-1.2M at 25 °C) vs Maxwell model, as discussed in the text. (b) Longitudinal modes ($Z = 1000$) proposed in the Likhtman−McLeish model vs Maxwell model, as discussed in the text.

value for the terminal peak is 3.56.[21,28] Lin[16] has previously assumed that the stress decay toward equilibrium by chain sliding motions is characterized by a single exponential (Maxwell form):

$$G(t) = \exp\left(-\frac{t}{\tau_X}\right) \tag{5}$$

where τ_X is the characteristic relaxation time. When a Maxwell loss modulus peak is shifted to superimpose on the reequilibration peak, a good agreement is observed, as shown in Figure 4a. However, to confirm the Maxwellian shape, it is important to also compare the experimental and predicted transitions for G'. This is more complicated since the monomer redistribution relaxation only represents a very small contribution to G'. In order to obtain the net contribution of the reequilibration transition, we first subtract G_N^0 from the experimental storage modulus, as the contribution of terminal relaxations. The resulting "low-frequency subtracted" storage modulus $G' - G_N^0$ runs almost parallel to G'' in the power law region. Next, the contribution of high-frequency relaxation on G' can be removed by subtracting a power law with the experimental exponent 0.71 from $G' - G_N^0$ (as was done for G''). It is worth noting that the observed scaling behavior of $G' - G_N^0$ and G'' in the power law region is rather consistent with the prediction of the Zimm model[29] ($^2/_3$ as opposed to the Rouse scaling $^1/_2$). This is also true for the ratio $G''/(G' - G_N^0)$, which is equal to 1.9, quite close to the Zimm prediction of $\sqrt{3}$.[1,7] The net reequilibration storage modulus transition is plotted in Figure 4a along with the corresponding loss modulus peak. Again, a good agreement with the Maxwell shape is observed, which is a logical consequence of the Kronig−Kramers relation but also confirms the consistency of the data and subtraction procedures used.

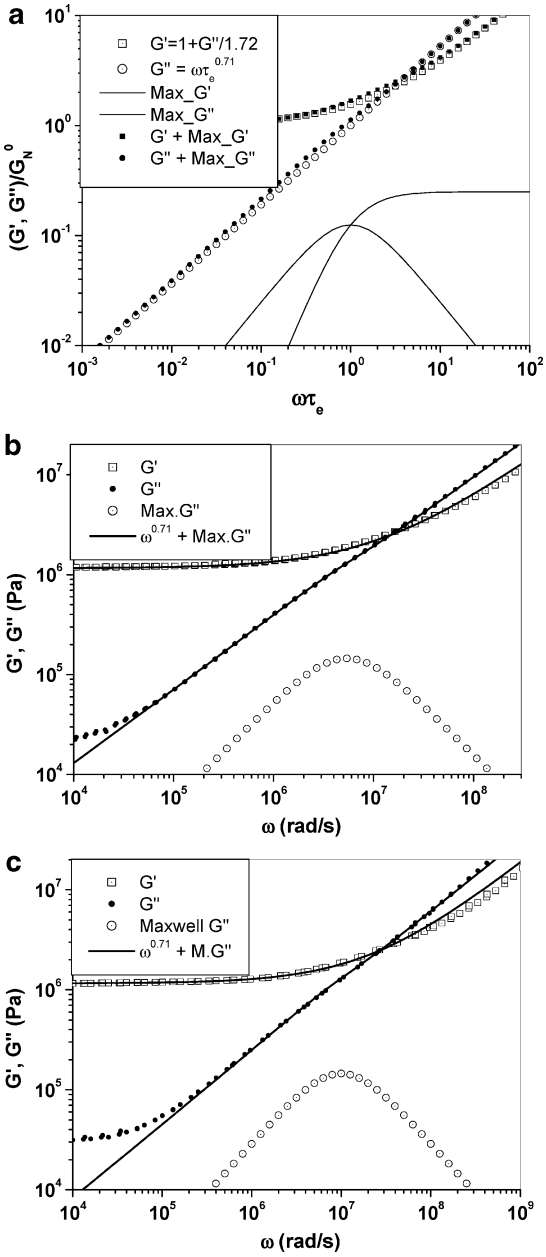

Figure 5. (a) Reconstruction of high-frequency relaxation modes by eqs 7 and 11, as discussed in the text. (b) Comparison of G' and G'' curves for PBD-1.2M and predictions of eq 11. Two material parameters are $G_N^0 = 1.16$ MPa and $\tau_e = 1.8 \times 10^{-7}$s. (c) Comparison of G' and G'' curves for PBD-410K and predictions of eq 11. Two material parameters are $G_N^0 = 1.16$ MPa and $\tau_e = 1.0 \times 10^{-7}$s.

DE[7] or Likhtman and McLeish[12] calculate that the longitudinal modes relax $^1/_5$ of the stress between τ_e and τ_R through a limited Rouse spectrum relaxation:

$$G(t) = \frac{1}{5Z}\sum_{p=1}^{Z} \exp\left(-\frac{p^2 t}{\tau_R}\right) \tag{6}$$

Figure 4b shows the result of eq 6 for $\tau_R = 1$s and $Z = 1000$ (hence $\tau_e = 10^{-6}$s). The peak of the corresponding G'' relaxation is located around $1/(3\tau_e)$ but is very broad and tails all the way down to $1/\tau_R$. This shape can be compared to the Maxwell peak with the same maximum frequency (lines in Figure 4b). The difference between the two shapes is very evident. The narrow experimental reequilibration peak following a Maxwell shape implies the reequilibration dynamics may only involve "a few"

Downloaded by UNIV CATHOLIQUE DE LOUVAIN on October 15, 2009 | http://pubs.acs.org
Publication Date (Web): March 24, 2007 | doi: 10.1021/ma062695f

Table 2. τ_e Evaluated by Different Methods for 1,4-PBD

method	related parameter	$\tau_e \times 10^7$ (s)	ref and (ref of data)
Rouse model fitting dynamic data	$\zeta_0 = 1.8 \times 10^{-7}$ g/s	5.9	1
kinematic viscosity	$\zeta_0 = 1.1 \times 10^{-7}$ g/s	3.6	31
kinematic viscosity	$\zeta_0 = 2.6 \times 10^{-7}$ g/s	8.5	24
tube model fitting data of star PBD	$\zeta_0 = 0.85 \times 10^{-7}$ g/s	5.1	34
tube model fitting data of linear PBD		4 or 4.9	12 (35)
		2.9	12 (36)
tube model calculation	$\tau_{rep} \sim 0.2$ s	~0.56	37 (24)
$\omega_{G''-G_N^0}$ cross point	5.4×10^6 rad/s	1.8	(PBD 1.2 M)
	$\sim 6 \times 10^6$ rad/s	1.7	(24)
	$\sim 3 \times 10^6$ rad/s	3.3	(35)
	$\sim 5 \times 10^6$ rad/s	2	(36)
	9.7×10^6 rad/s (at 40 °C)	2 at 25 °C (1 at 40 °C)	(PBD 410K, 23)

entanglement segments and not the entire chain. For significantly longer segments than the entanglement length, a power law behavior is apparently recovered, with the same exponent as the one observed above the crossover, i.e. for segments shorter than the entanglement length.

Fitting of the High-Frequency Relaxation Region. We take advantage of the complete isolation of the terminal relaxation, on the one hand, and the clear superposition of a power law and Maxwell relaxation at high frequencies, on the other hand, to empirically model the rheological response of PBD-1.2M in the region extending on both sides of the second crossover (below the glassy-dominated region and above the fluctuations dominated region). The total response can be split into independent contributions[30] and written as

$$G^*_{total}(\omega) = G^*_{term}(\omega) + G^*_{high-freq}(\omega) + G^*_{re-eq}(\omega) \quad (7)$$

where $G**_{term}$, $G^*_{high-freq}$, and G^*_{reeq} are the respective contributions of the low-frequency terminal relaxations, high-frequency power law relaxation and monomer redistribution relaxation to the total modulus G^*_{total}.

The low-frequency relaxation can be approximated (in the region of interest) by a constant elastic contribution equal to the plateau modulus:

$$G'_{term}(\omega) = G_N^0 \quad (8)$$
$$G''_{term}(\omega) = 0$$

The power law observed in a very broad region (over 3 decades in Figure 1a or 3a) extending on both sides of the monomer redistribution relaxation can be represented as

$$G'_{high-freq}(\omega) \cong G_N^0(\omega\tau_e)^\alpha/1.72 \quad (9)$$
$$G''_{high-freq}(\omega) \cong G_N^0(\omega\tau_e)^\alpha$$

with α varying slightly from 0.68 to 0.71 depending on the polymer tested. The numerical factor ~1.72 is consistent with the exponent of the power law and works for all the samples. We assume $G''_{high-freq}(1/\tau_e) = G_N^0$ as a reasonable experimental definition for the basic relaxation time τ_e, (refer to Figure 3a).

Finally, the monomer reequilibration dynamics $G^*_{re-eq}(\omega)$ is described by a Maxwell relaxation, in accordance with the experimental findings:

$$G'_{re-eq}(\omega) = \frac{1}{4}G_N^0\frac{(\omega\tau_e)^2}{1+(\omega\tau_e)^2} \quad (10)$$

$$G''_{re-eq}(\omega) = \frac{1}{4}G_N^0\frac{\omega\tau_e}{1+(\omega\tau_e)^2}$$

Here, the relaxation strength is $^1/_4$ of G_N^0, and the characteristic relaxation time is equal to the basic relaxation time τ_e (Table 1).

The total storage modulus G' and loss modulus G'' at high frequencies can thus be written as

$$G'_{total}(\omega) = G_N^0\left(1 + \frac{(\omega\tau_e)^\alpha}{1.72} + \frac{1}{4}\frac{(\omega\tau_e)^2}{1+(\omega\tau_e)^2}\right) \quad (11)$$

$$G''_{total}(\omega) = G_N^0\left((\omega\tau_e)^\alpha + \frac{1}{4}\frac{\omega\tau_e}{1+(\omega\tau_e)^2}\right)$$

Figure 5a shows the fitting of the data by eq 11. $G^*_{term}(\omega) + G^*_{high-freq}(\omega)$ are displayed as open symbols. Filled symbols represent the total relaxation modulus. The reequilibration relaxation $G^*_{re-eq}(\omega)$ is shown as lines.

To fit this simple model to the experimental data in Figure 3a, two material parameters are required: the plateau modulus G_N^0 and the equilibration time τ_e. G_N^0 is taken as 1.16 MPa in agreement with the consensus value.[21] For the horizontal scale, we shift the calculated G' and G'' curves to overlap with the experimental results for PBD-1.2M (Figure 5b). This sets the actual value of τ_e. The agreement between the experimental results and predictions is excellent in the high-frequency region. The calculated moduli almost perfectly capture the relaxation dynamics in the entire transition region. It is worth noting that the horizontal shift factor is 5.4×10^6, corresponding τ_e is 1.8×10^{-7}s, agrees with the results of tube model within a factor of about 3.[12,22] When the same procedure is applied to PBD-410K, the agreement between the data of and predictions is also good, as shown in Figure 5c. The only difference is the horizontal shift factor, equal to 10×10^6 (corresponding $\tau_e = 1.0 \times 10^{-7}$s), since the reference temperature for the master curve is now 40 °C.[23] See also Appendix A.

Conclusions

The monomer density reequilibration relaxation is directly observed for the first time from the linear viscoelastic data of very high MW PBD, PI, PIB samples. We use a simple procedure of subtracting contributions of the high-frequency power law relaxation from the experimental curves with an experimental exponent close to 0.7. The stress decay of the monomer redistribution process is characterized by a single exponential (Maxwell form), and the relaxation strength observed is 1/4 of the plateau modulus G_N^0. Moreover, the characteristic relaxation time is close to the equilibration time

Downloaded by UNIV CATHOLIQUE DE LOUVAIN on October 15, 2009 | http://pubs.acs.org
Publication Date (Web): March 24, 2007 | doi: 10.1021/ma062695f

τ_e. The observed reequilibration dynamics appear to be independent of polymer species.

The high-frequency relaxation modes can be reconstructed as a superposition of high-frequency power law relaxation and Maxwell monomer reequilibration. The calculated G' and G'' curves show excellent agreement with the experimental results over the high-frequency region. It is clear that the proposed superposition (i.e., distinction) between power law and Maxwell relaxations around τ_e is at odds with current ideas about Rouse motions in a tube, as developed for instance in the Likhtman−McLeish theory.[12] However, current tube models do not correctly predict the observed slope and therefore the proposed superposition, although empirical, can be considered as an alternative description. In addition, we propose a possible "experimental definition" for the basic relaxation time τ_e. It corresponds to an easily observable point ($G''(1/\tau_e) = G_N^0$), at least for highly entangled samples.

Acknowledgment. This work has been supported by an ARC grant from the "Communauté française de Belgique" (CYL). We are grateful to Prof. S. Q. Wang for providing access to experimental data. We also thank Dr A.E. Likhtman and Prof. W. W. Graessley for their valuable comments.

Downloaded by UNIV CATHOLIQUE DE LOUVAIN on October 15, 2009 | http://pubs.acs.org
Publication Date (Web): March 24, 2007 | doi: 10.1021/ma062695f

Appendix A. Summary of τ_e values reported in literature for 1,4-PBD

The values of the Rouse time of an entanglement strand at 25 °C reported in literature are listed in Table 2. The comparison of the literature values for τ_e needs to consider the consistency of the definition, the material parameters and the temperature.

Ferry[1] deduces the monomer friction coefficient, ζ_0, from dynamic measurements in the transition region. The parameter ζ_0, is also evaluated from the Rouse model expression for kinematic viscosity by Roovers[31] and Colby et al.,[24] respectively. The values of ζ_0 are transformed to τ_e by the expression:

$$\tau_e = \left(\frac{M_e}{M_0}\right)^2 \frac{\zeta_0 b^2}{3\pi^2 k_B T} \tag{12}$$

Here $M_e = 1570$ g/mol, $M_0 = 54$ g/mol, and $b = 0.688$ nm. We use this particular value for M_e because it is convenient for comparison with results obtained by tube model fitting. Likhtman and McLeish[12] use the definition of M_e with the 4/5 prefactor (for the definition of entanglement spacing, see also the paper of Larson et al.[32]). For the statistical segment length b, the value comes from $b^2/M_0 = \langle R^2\rangle_0/M = 0.876$ Å^2 mol/g listed in the Fetters and co-workers review paper.[33]

It is worth noting that Colby et al. adjust the viscosity of low molecular weight PBD samples to the iso-free-volume state of the high molecular weight samples. The correction accounts for a factor 2 difference in friction coefficient. The value of ζ_0 or τ_e (the maximum in Table 2) reported in Colby's paper are probably too high, because the corresponding predicted line in Figure 7 of ref 24 for $G'$and G'' by the Rouse model not only has the wrong slope, but also is biased toward low frequency (hence long relaxation times).

Vega et al.[34] fit the viscosity data of star PBD with the help of the Milner−McLeish model to obtain ζ_0. However, since τ_e and M_e are fitting parameters in their paper, the value of ζ_0 was actually obtained from τ_e with the help of eq 12 by using the fitted M_e value (2120 g/mol). The true value of τ_e, which must be recovered from ζ_0 with the same M_e and is 5.1×10^{-7} s.

Likhtman and McLeish[12] fit the LVE data of linear PBD to obtain τ_e with the help of their tube model with contour-length fluctuations and constraint release corrections. They use the dynamic measurements reported by Baumgaertel et al.,[35] Juliani and Archer.[36]

Rubinstein and Colby[37] calculate τ_e, from the experimental reptation time of the chain $\tau_{rep} = 0.2$ s with the help of the tube model:

$$\frac{\tau_{rep}}{\tau_e} = 6\left(\frac{M}{M_e}\right)^3 \tag{13}$$

They use the dynamic rheological data measured by Colby et al.[24] and $M_e = 1900$ g/mol for the calculation. The corresponding value of τ_e of about 1×10^{-7} s must be adjusted to 0.56×10^{-7} s if we use $M_e = 1570$ g/mol for consistency with the other data in Table 2. The value is very low. A possible reason is that authors use the original reptation model and do not consider contour-length fluctuation and constraint release effects. We also notice the definition in the paper of Larson et al.[32] is $\tau_{rep}/\tau_e = 3(M/M_e)^3$. All possible corrections will increase the value of τ_e.

Clearly, literature values evaluated by different methods differ by a factor larger than 3.

The "experimental definition" for τ_e proposed in the paper, corresponding to an easily observable cross-point frequency between the extended plateau modulus and the power law region of the loss modulus, provides a convenient method for a model-independent experimental determination of τ_e. The values obtained from different sources[23,24,35,36] are quite consistent (within a factor of 2), when the data at 40 °C are converted to 25 °C.

References and Notes

(1) Ferry, J. D. *Viscoelastic Properties of Polymers*; Wiley: London, 1980.
(2) Graessley, W. W. *Adv. Polym. Sci.* **1974**, *16*, 1.
(3) Watanabe, H. *Prog. Polym. Sci.* **1999**, *24*, 1253.
(4) McLeish, T. C. B. *Adv. Phys.* **2002**, *51*, 1379.
(5) van Ruymbeke, E.; Bailly, C.; Keunings, R.; Vlassopoulos, D. *Macromolecules* **2006**, *39*, 6248.
(6) De Gennes, P. G. *J. Chem. Phys.* **1971**, *55*, 572. De Gennes, P. G. *Scaling Concepts in Polymer Physics*; Cornell University Press: Ithaca, NY, 1979.
(7) Doi, M.; Edwards, S. F. *The Theory of Polymer Dynamics*; Clarendon Press: Oxford, U.K., 1986.
(8) Liu, C. Y.; Keunings, R.; Bailly, C. *Phys. Rev. Lett.* **2006**, *97*, 246001.
(9) Marrucci, G. *J. Polym. Sci., Polym. Phys. Ed.* **1985**, *23*, 159.
(10) Rubinstein, M.; Colby, R. H. *J. Chem. Phys.* **1988**, *89*, 5291.
(11) Doi, M. *J. Polym. Sci., Polym. Lett. Ed.* **1981**, *19*, 265. Doi, M. *Polym. Phys. Ed.* **1983**, *21*, 667.
(12) Likhtman, A. E.; McLeish, T. C. B. *Macromolecules* **2002**, *35*, 6332.
(13) Rouse, P. E. *J. Chem. Phys.* **1953**, *21*, 1272.
(14) Treloar, L. R. G. *The Physics of Rubber Elasticity*, 2nd ed.; Oxford University Press: London, 1958. (b) Mark, J. E. *J. Am. Chem. Soc.* **1970**, *92*, 7252.
(15) Ball, R. C.; Doi, M.; Edwards, S. F.; Warner, M. *Polymer* **1981**, *22*, 1010. (b) Edwards, S. F.; Vilgis, T. *Polymer* **1986**, *27*, 483.
(16) Lin, Y. H. *Macromolecules* **1984**, *17*, 2846.
(17) Milner, S. T.; McLeish, T. C. B. *Phys. Rev. Lett.* **1998**, *81*, 725.
(18) Rubinstein, M.; Panyukov, S. *Macromolecules* **2002**, *35*, 6670.
(19) Masubuchi, Y.; Ianniruberto, G.; Greco, F.; Marrucci, G. *J. Chem. Phys.* **2003**, *119*, 6925.
(20) Liu, C. Y.; Bailly, C.; Yao, M.; Garritano, R. G.; Franck, A. J. Instrument Compliance Problems Revisited: Linear Viscoelasticity Measurements. Submitted to *J. Rheol.*
(21) Liu, C. Y.; He, J. S.; Keunings, R.; Bailly, C. *Polymer* **2006**, *47*, 4461.
(22) Liu, C. Y.; Halasa, A. F.; Keunings, R.; Bailly, C. *Macromolecules* **2006**, *47*, 7215.
(23) Wang, S.; Wang, S. Q.; Halasa, A.; Hsu, W. L. *Macromolecules* **2003**, *36*, 5355.
(24) Colby, R. H.; Fetters, L. J.; Graessley, W. W. *Macromolecules* **1987**, *20*, 2226.

(25) Smith, G. D.; Paul, W.; Monkenbusch, M.; Richter, D. *J. Chem. Phys.* **2001**, *114*, 4285.
(26) Harnau, L.; Winkler, R. G.; Reineker, P. *Phys. Rev. Lett.* **1999**, *82*, 2408.
(27) van Meerveld, J. *Rheol. Acta* **2004**, *43*, 615.
(28) Raju, V. R.; Menezes, E. V.; Marin, G.; Graessley, W. W.; Fetters, L. J. *Macromolecules* **1981**, *14*, 1668.
(29) Zimm, B. H. *J. Chem. Phys.* **1956**, *24*, 269.
(30) Kapnistos, M.; Vlassopoulos, D.; Roovers, J.; Leal, L. G. *Macromolecules* **2005**, *38*, 7852.
(31) Roovers, J. *Polymer* **1985**, *26*, 1091.
(32) Larson, R. G.; Sridhar, T.; Leal, L. G.; McKinley, G. H.; Likhtman, A. E.; McLeish, T. C. B. *J. Rheol.* **2003**, *47*, 809.
(33) Fetters, L. J.; Lohse, D. J.; Richter, D.; Witten, T. A.; Zirkel, A. *Macromolecules* **1994**, *27*, 4639.
(34) Vega, D. A.; Sebastian, J. M.; Russel, W. B.; Register, R. A. *Macromolecules* **2002**, *35*, 169.
(35) Baumgaertel, M.; De Rosa, M. E.; Machado, J.; Masse, M.; Winter, H. H. *Rheol. Acta* **1992**, *31*, 75.
(36) Juliani, Archer, L. A. *J. Rheol.* **2001**, *45*, 691.
(37) Rubinstein, M.; Colby, R. H. *Polymer Physics*; Oxford University Press: Oxford, U.K., 2003.

MA062695F

Downloaded by UNIV CATHOLIQUE DE LOUVAIN on October 15, 2009 | http://pubs.acs.org
Publication Date (Web): March 24, 2007 | doi: 10.1021/ma062695f